THE JOURNAL OF BIOLOGICAL CHEMISTRY
Vol. 275, No. 51, Issue of December 22, pp. 39954–39963, 2000
Printed in U.S.A.

Ca^{2+}-activated K^+ Channels in Human Leukemic Jurkat T Cells

MOLECULAR CLONING, BIOCHEMICAL AND FUNCTIONAL CHARACTERIZATION*

Received for publication, February 24, 2000, and in revised form, September 15, 2000
Published, JBC Papers in Press, September 15, 2000, DOI 10.1074/jbc.M001562200

Rooma Desai‡, Asher Peretz‡, Hirsh Idelson§, Philip Lazarovici¶, and Bernard Attali‡‖

From the ‡Department of Neurobiology, The Weizmann Institute of Science, 76100 Rehovot, Israel, §Alomone Labs, Jerusalem, 91042, Israel, and the ¶Department of Pharmacology and Experimental Therapeutics, School of Pharmacy, Faculty of Medicine, The Hebrew University of Jerusalem, Jerusalem 91120, Israel

Previous studies have demonstrated the presence of apamin-sensitive, small-conductance Ca^{2+}-activated K^+ currents in human leukemic Jurkat T cells. Using a combined cDNA and reverse transcriptase-polymerase chain reaction cloning strategy, we have isolated from Jurkat T cells a 2.5-kilobase cDNA, *hSK2*, encoding the human isoform of SK2 channels. Northern blot analysis reveals the presence of a 2.5-kilobase *hSK2* transcript in Jurkat T cells. While present in various human tissues, including brain, heart, skeletal muscle, kidney, and liver, no *hSK2* mRNA could be detected in resting and activated normal human T cells. The *hSK2* gene is encoded by 8 exons and could be assigned to chromosome 5 (q21.2-q22.1). The protein encoded by *hSK2* is 579 amino acids long and exhibits 97% identity with its rat counterpart rSK2. When expressed in Chinese hamster ovary cells, *hSK2* produces Ca^{2+}-activated K^+ currents with a unitary conductance of 9.5 pS and a $K_{0.5}$ for calcium of 0.7 μM; hSK2 currents are inhibited by apamin, scyllatoxin, and *d*-tubocurarine. Overexpression of the Src family tyrosine kinase $p56^{lck}$ in Jurkat cells, upregulates SK2 currents by 3-fold. While IKCa channels are transcriptionally induced upon activation of normal human T cells, our results show that in Jurkat cells SK2 channels are constitutively expressed and down-regulated following mitogenic stimulation.

Ca^{2+}-activated K^+ channels (KCa) represent a class of potassium channels that respond to changes in intracelluar Ca^{2+} concentration, and couple Ca^{2+} metabolism to K^+ flux and membrane excitability. Based on their electrophysiological properties, three main classes of KCa channels have been characterized (for review, see Refs. 1–3): the large conductance, Ca^{2+}- and voltage-gated channels (BK), the intermediate conductance, voltage-independent channels (IK), and the small conductance, voltage-independent channels (SK) (1–3). SK channels have unitary conductance of 4–14 pS, are voltage-independent and are activated in the range of 200–500 nM $[Ca^{2+}]_i$.[1] Some SK currents are blocked by apamin, an 18-mer peptide toxin from bee venom and by scyllatoxin, a 31-mer polypeptide scorpion toxin (4–7). In the brain, they are responsible for the slow after hyperpolarizing phase of action potentials which modulates the firing pattern of neurons (1–3). SK channels are also expressed in a wide variety of peripheral tissues including adrenal cortex, liver, skeletal, and smooth muscles as well as leukemic Jurkat T cells (8–19).

Human T lymphocytes are endowed with at least two different types of K^+ channels, voltage-gated K^+ channels (Kv) and KCa channels (for review, see Ref. 20). The Kv channel in human T cells has been characterized extensively at the physiological and molecular levels (20). It is encoded by *hKv1.3*, a *Shaker*-related Kv channel gene (21, 22). Two KCa channel subtypes have been characterized in lymphocytes and lymphocytic cell lines. The predominant KCa channel found in normal human peripheral T cells has a 15–40 pS unitary conductance, is a charybdotoxin (CTX)-sensitive and apamin-insensitive inwardly-rectifying channel that is also known as intermediate conductance (IK) (23, 24). A gene encoding IK, called *hSK4* (or *hIK1, hIKCa1*, and *hKCa4*) has been recently cloned from various human tissues (25–28). The prominent KCa channel expressed in the human leukemic Jurkat T cell line corresponds to an apamin-sensitive, small-conductance channel (4–7 pS) (16, 17). Recent work (29) showed that *SK2* encodes this KCa current based on the PCR amplification of a partial Jurkat *SK2* cDNA fragment.

Three genes encoding SK channel family members have been cloned from human (*hSK1*) and rat brains (*rSK2* and *rSK3*) (30). These different isoforms encode the pore-forming α subunit of SK channels and exhibit a high degree of sequence identity with 70–80% amino acid sequence identity. Hydrophobicity analysis predicts a *Shaker*-like structure (30). Recent studies revealed that Ca^{2+} gating involves the constitutive association of calmodulin with a C-terminal domain of SK channel α subunits (31–34). Some cloned isoforms of SK channels are blocked by apamin and by *d*-tubocurarine (dTC), a plant alkaloid (29, 35–37). The residues Asp^{341} and Asn^{368} on either side of the deep pore of the α subunit were shown to be the primary determinants of apamin and dTC sensitivity (35).

* This work was supported in part by grants from the Minerva Foundation, the Israel Science Foundation, the Israel Ministry of Health, and the Israel Cancer Research Fund (RCDA). The costs of publication of this article were defrayed in part by the payment of page charges. This article must therefore be hereby marked "*advertisement*" in accordance with 18 U.S.C. Section 1734 solely to indicate this fact.

The nucleotide sequence reported in this paper for the human hSK2 sequence (KCNN2) has been submitted to the GenBank™/EBI Data Bank with accession number AF239613.

‖ Incumbent of the Philip Harris and Gerald Ronson Career Development Chair. To whom correspondence should be addressed: Dept. of Neurobiology, The Weizmann Institute of Science, Rehovot 76100, Israel. Tel.: 972-89-342315; Fax: 972-89-344131; E-mail: bernard.attali@weizmann.ac.il.

[1] The abbreviations used are: KCa, Ca^{2+}-activated K^+ channels; SK, small conductance Ca^{2+}-activated K^+ channels; dTC, *d*-tubocurarine; BK, large-conductance Ca^{2+}- and voltage-gated K^+ channels; IK, the intermediate conductance Ca^{2+}-activated K^+ channels; Kv, voltage-gated K^+ channels; CTX, charybdotoxin; LCK^-, $p56^{lck}$-deficient Jurkat cells; LCK^+, $p56^{lck}$-overexpressing Jurkat cells; DTX, α-dendrotoxin; ORF, open reading frame; PHA, phytohemagglutinin A; $[Ca^{2+}]_i$, intracellular $[Ca^{2+}]$; PCR, polymerase chain reaction; kb, kilobase(s); CHO, Chinese hamster ovary; bp, base pair(s); UTR, untranslated region; RT-PCR, reverse transcriptase-polymerase; EST, expressed sequence tag; PHA, phytohemagglutinin A; TPA, 12-*O*-tetradecanoylphorbol-13-acetate; HTGS, high-throughput genome sequence.

In this study, we cloned from human Jurkat T cells a 2.5-kb full-length cDNA, *hSK2*, encoding the human isoform of SK2 channels. While *hSK2* transcripts are found in various human tissues, including brain, heart, skeletal muscle, kidney, and liver, no *hSK2* mRNA could be detected in normal human T cells. Based on high-throughput genome sequence analysis (HTGS), we show that the *hSK2* gene is encoded by 8 exons and could be assigned to human chromosome 5 (q21.2-q22.1). Similar to native Jurkat KCa currents, *hSK2* produces in transfected mammalian cells a time- and voltage-independent Ca^{2+}-activated K^+ current which is inhibited by apamin, scyllatoxin, and dTC. In Jurkat cells overexpressing the Src family tyrosine kinase $p56^{lck}$ (LCK^+), the SK2 channel activity increases by more than 3-fold. In contrast to IKCa channels which are transcriptionally induced upon activation of normal human T cells, our data show that in Jurkat cells, SK2 channels are constitutively expressed and are down-regulated following mitogenic stimulation.

EXPERIMENTAL PROCEDURES

Cells—Human leukemic Jurkat T cells and the $p56^{lck}$-deficient Jurkat cells (LCK^-) were maintained in RPMI culture medium supplemented with 2 mM glutamine, antibiotics, and 10% fetal calf serum in a humidified, 5% CO_2 incubator at 37 °C. The $p56^{lck}$-overexpressing Jurkat cells (LCK^+) were generated from LCK^- cells which were retransfected with $p56^{lck}$ tyrosine kinase and were maintained in the above medium supplemented with hygromycin B (Roche Molecular Biochemicals, 100 μg/ml). Rat pheochromocytoma PC12 cells were maintained in Dulbecco's modified Eagle's medium supplemented with 2 mM glutamine, 8% horse serum, 10% fetal calf serum and antibiotics. HEK 293 and CHO cells were maintained in Dulbecco's modified Eagle's medium supplemented with 2 mM glutamine, 10% fetal calf serum and antibiotics in a humidified, 5% CO_2 incubator at 37 °C.

Electrophysiology—Human leukemic T cell line Jurkat, LCK^-, LCK^+, hSK2-transfected CHO and HEK 293 cells were plated on poly-L-lysine-coated coverslips settled on a 1.5-ml chamber, mounted on the stage of an Axiovert 35 inverted microscope (Carl Zeiss). Recordings were made at 22 ± 1 °C, using patch pipettes pulled from borosilicate glass capillaries (fiber filled) with resistance of 4–8 MΩ. Patch clamp recordings were performed using standard techniques (38). For whole cell patch clamp recordings, two different solutions were used, external high $[K^+]$ and physiological solutions. In the external high K^+ solutions, the patch pipette contained (in mM): 135 K aspartate, 40 KOH, 2 $MgCl_2$, 10 HEPES, 10 EGTA, and 8.7 $CaCl_2$ (1 μM free Ca^{2+}) adjusted to pH 7.2 with KOH, while the bath solution contained (in mM): 165 KCl, 2 $CaCl_2$, 2 $MgCl_2$, and 10 HEPES, adjusted to pH 7.2 with KOH. For the physiological solutions, the patch pipette contained (in mM): 110 K gluconate, 20 KCl, 1 $MgCl_2$, 5 KATP, 10 HEPES, 5 EGTA, and 4.7 $CaCl_2$ (1 μM free Ca^{2+}) adjusted to pH 7.4 with KOH, while the bath solution contained (in mM): 140 NaCl, 5 KCl, 1.8 $CaCl_2$, 1.2 $MgCl_2$, 11 glucose, and 5.5 HEPES, adjusted to pH 7.4 with NaOH. For inside-out patch clamp recording, the pipette solution (out) contained (in mM): 144 KCl, 2 $CaCl_2$, 1 $MgCl_2$, 10 HEPES, adjusted to pH 7.2 with KOH and 2 mM sucrose; the bath solution (in) contained (in mM): 150 KCl, 40 KOH, 1 $MgCl_2$, 8.2 $CaCl_2$ (0.77 μM free Ca^{2+}), 10 EGTA, and 10 HEPES, adjusted to pH 7.2 with KOH. Solutions were adjusted with sucrose at ~300–315 mosmol $liter^-$. Series resistance were compensated by 85–95%. Signals were amplified using an Axopatch 200B patch clamp amplifier (Axon Instruments) and filtered at 1–2 KHz, via a 4-pole Bessel filter. Data were sampled at 2.5–10 KHz and analyzed using pClamp 6.0.2 software (Axon Instruments) on an IBM-compatible 486 computer interfaced with DigiData 1200 (Axon Instruments). Further data analysis was done using Axograph 3.0 software (Axon Instruments) and Excel 5.0 (MicroSoft) on an Apple MacIntosh computer.

Membrane Preparation and Western Blotting—Cells were harvested and washed twice in cold phosphate-buffered saline and were then resuspended (1.5×10^7 cells/ml) in cold homogeneization buffer (50 mM Tris-HCl, pH 7.4, 1 mM EDTA, and 1 mM phenylmethylsulfonyl fluoride, 10 μg/ml leupeptin, and 10 μg/ml aprotinin). Cells were homogenized with a Teflon glass homogenizer and the homogenate was centrifuged at 1,000 × *g* for 5 min (at 4 °C) to remove large cell debris. The supernatant was centrifuged at 21,000 × *g* for 30 min (at 4 °C) and the membrane pellet (crude membrane fraction) was resuspended in cold homogeneization buffer and sonicated for 30 s. The membrane homogenates were then aliquoted, quickly frozen in liquid nitrogen and stored at −70 °C until use. Western blots were performed as described (39). Polyclonal anti-rat SK2 antibodies and anti-human Kv1.3 antibodies (Alomone labs) were used at 1.5 μg/ml.

Transfections—For electrophysiological recording, CHO and HEK 293 cells were transfected with *hSK2* subcloned into the pCDNA3 vector (Invitrogen). Cells were seeded (5.10^4 cells/well) on poly-L-lysine-coated glass coverslips in 24-multiwell plates. Transfection was performed according to the manufacturer's protocol (Life Technologies, Inc.) using 1.5 μl of LipofectAMINE and 0.25 μg of hSK2-pCDNA3 together with 0.5 μg of pIRES-CD8 (kindly provided by Drs. J. Barhanin and A. Patel, CNRS, Sophia Antipolis, France), as a marker for transfection. Transfected cells were visualized 48 h following transfection, using the anti-CD8 (Dynal) antibody-coated beads method (40).

Molecular Cloning of hSK2—Total RNA from Jurkat T cells was isolated as described (41) and poly(A^+) RNA was isolated using oligo(dT)-Sepharose (Collaborative Research). Single-stranded cDNA was synthesized from 5 μg of total RNA or 250 ng of poly(A^+) RNA using 200 units of Superscript II™ RNase H^- reverse transcriptase (Life Technologies, Inc.). The cDNA was primed either with the tagged oligo(dT) primer 5′-CCAGTGAGCAGAGTGACGAGGACTCGAGCTCAAGCTTT-TTTTTTTTTTTTT-3′ or with random primers. The single-stranded cDNA was used as a template for PCR. Degenerate primers were designed on the basis of the homology between the different SK channel isoforms: *rSK1, rSK2, rSK3*, and *hSK1*. The primers 5′-ATHTTYGG-NATGTTYGGNA-3′ (primer A) and 5′-CCACATNGCNCCNARRAART-T-3′ (primer B), were used to PCR amplify from Jurkat T cells the initial 633-bp fragment of *hSK2*. All PCR reactions were performed using the proof reading *Pfu* DNA polymerase (Promega). The sequence was further extended by a 5′ and 3′ rapid amplification of cDNA ends-PCR cloning strategy (42) and a poly(A)-tailed cDNA fragment of 2166 bp length was obtained. A blastn search of the GenBank™ data base at the National Center for Biotechnology Information was performed. Human expressed sequence tags overlapping the 5′ (EST: AI339865 and AI271784) and 3′ (EST: AI700829 and AI680869) untranslated regions of our 2166-bp cDNA were found. The EST AI339865 further extended the 5′-UTR sequence by 343 bp. The whole cDNA sequence of 2509 bp was amplified by RT-PCR from Jurkat mRNA confirming the co-linearity of the overlapping cDNA fragments.

Northern Blot Analysis—Human 12-lane multiple tissue and Human Cancer Cell Line MTN™ blots (CLONTECH) were used. For Jurkat cells, 5 μg of mRNA were resolved by electrophoresis on a 1 M formaldehyde, 1% agarose gel and then blotted overnight onto a Hybond-N membrane (Amersham) in 20 × SSC (3 M sodium chloride, 0.3 M sodium citrate, pH 7.0). The Northern blots were probed with a [^{32}P]dCTP-labeled 660-bp DNA probe spanning the extreme C-terminal region (including the 3′-UTR) of the *hSK2* cDNA. Another 5′ specific *hSK2* probe which consisted in the whole 456-bp 5′-UTR, was used to check the specificity of the Northern signals. Hybridization was carried out at 68 °C for 1 h using the solutions (CLONTECH) and according to the manufacturer's protocol (CLONTECH). Signal was visualized with a PhosphorImager 445 SI, after 16–23 h exposure.

RESULTS

Human Leukemic Jurkat T Cells Express Apamin- and dTC-sensitive SK Currents—Jurkat T cells are known to express both Kv and SK currents (16, 17). To identify SK currents, we used the whole cell configuration of the patch clamp technique. SK channels were activated by employing a high capacity Ca^{2+}-buffered pipette solution at free $[Ca^{2+}]_i$ of 1 μM. Currents were recorded in external high K^+ solutions (165 mM K^+, see "Experimental Procedures"), using voltage ramps of 400 ms from −160 to +40 mV, to identify both Kv and SK currents (Fig. 1, *A* and *B*). Under these experimental conditions, Kv currents activated at potentials positive to −40 mV leading to inward currents below and outward currents above 0 mV. SK currents were clearly identified at potentials below −50 mV, as the SK channel slope conductance increased at negative potentials, while that of Kv is minimal. Similar Kv and SK current components were previously described using the same recording solutions (16, 17). Fig. 1*D* shows the same SK current recorded, using a different protocol in which cells were stepped from −120 to −10 mV from a 0-mV holding potential. Note that at very negative potentials, the SK current is partially contaminated by the deactivating tail of the Kv1.3 current which does

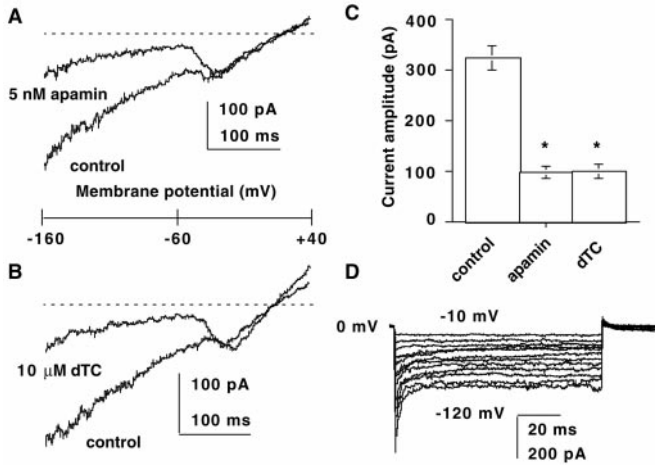

FIG. 1. **Pharmacology of SK currents in Jurkat cells.** *A* and *B*, ramp currents before and after 5 nM apamin (*A*) and 10 μM dTC (*B*). From a holding potential of 0 mV, cells were subjected to a ramp of 400 ms from −160 to +40 mV. The *dotted line* represents the zero current level. *C*, current amplitude as measured at −140 mV (pA ± S.E.) in cells before (control, $n = 22$) and after exposure to apamin (5 nM, $n = 13$) and dTC (10 μM, $n = 10$). Results are statistically significant (* $p < 0.01$). *D*, from a holding potential of 0 mV, cells were stepped for 100 ms from −120 to −10 mV in 10-mV increments. SK currents were recorded in external high K^+ solutions.

not totally inactivate at a holding potential of 0 mV. In agreement with previous work (17), we found that apamin (5 nM) and dTC (10 μM) inhibit Jurkat SK currents by 70% (Fig. 1, *A-C*). In contrast, this current is insensitive to 100 nM CTX and 100 nM DTX (data not shown).

Molecular Cloning of hSK2 in Jurkat T Cells—To identify unambiguously the molecular isoform encoding the Jurkat SK channel, degenerate primers were designed based on the homology existing between the previously cloned SK channels *rSK1, rSK2, rSK3*, and *hSK1* (30) and an RT-PCR was performed. The primers spanning the middle of the S1 segment (primer A) and the N-terminal boundary of the pore domain (primer B, see Fig. 2 and "Experimental Procedures") amplified an initial cDNA fragment of 633 bp, which was highly homologous to *rSK2*. The sequence was further extended by a 5′ and 3′ rapid amplification of cDNA ends-PCR cloning strategy (42) and a poly(A)-tailed cDNA fragment of 2166 bp length was obtained. A blastn search of the GenBank™ data base at the National Center for Biotechnology Information was performed. A human expressed sequence tag (EST AI339865) overlapping the 5′-untranslated region of our 2166-bp cDNA was found. This EST further extended the 5′-UTR sequence by 343 bp. The whole cDNA sequence of 2509 bp was amplified by RT-PCR from Jurkat mRNA and sequenced, confirming the co-linearity of the overlapping cDNA fragments. Thus, the whole cDNA obtained (2509 bp) probably corresponds to the full-length mRNA in Jurkat T cells since in Northern blots, a 2.5-kb transcript was detected (Fig. 3*A*). Neither SK1 nor SK3 could be amplified from Jurkat cDNA (Ref. 29, and not shown).

The Jurkat cDNA which we termed *hSK2*, corresponds to the human isoform of the rat *rSK2* sequence. It comprises an open reading frame of 1737 bp (nucleotide position 457–2193), a 456-bp 5′-UTR and a 333-bp 3′-UTR ended with a polyadenylation signal and a poly(A^+) tail. The putative initiation codon has a Kozak consensus sequence GCCATGA (43), although we did not detect an in-frame stop codon upstream the initiator ATG (nucleotide position 457). The protein encoded by *hSK2* is 579 amino acids long and exhibits 97% identity with its rat protein counterpart *rSK2* (Fig. 2). Except for the N terminus which exhibits minor differences between *hSK2* and *rSK2* (amino acids 51–54 and 99–102), the protein sequences are virtually identical for both species (Fig. 2). The predicted hSK2 protein contains several consensus cAMP-dependent protein kinase, casein kinase II and protein kinase C phosphorylation sites at the N and C termini. Like *rSK2, hSK2* does not possess *N*-glycosylation sites at predicted extracellular locations.

Tissue Distribution, Phylogenetic Tree, and Chromosomal Localization—Northern blot analysis performed in various human tissues reveals a major 2.5-kb *hSK2* transcript in Jurkat T cells, liver, kidney, and brain with the strongest signals in liver and brain (Fig. 3*A*). Higher molecular weight transcripts (4.4 kb) were found in heart and skeletal muscle, while a lower mRNA species (1.3 kb) was also observed in brain and liver (Fig. 3*A*). The 4.4-kb transcript may represent a cross-reactive mRNA species from the SK channel family although a 5′ specific *hSK2* probe which consisted in the whole 456-bp 5′-UTR, was used to check the specificity of the Northern signals (Fig. 3*A*). No detectable transcripts were observed in small intestine, placenta, lung, thymus, spleen, and normal peripheral T cells (Fig. 3*A* and see also, Fig. 7*C*). Interestingly, *hSK2* is expressed in melanocytes (EST AA418096) and fetal heart (EST AA418000). Since *hSK2* is not expressed in normal spleen, thymus, and peripheral T cells, we checked for the presence of *hSK2* mRNA in some human tumor cell lines to test whether the expression of SK2 is a marker of certain T-cell malignancies. No *hSK2* transcript was detected in promyelocytic leukemia HL-60, HeLa S3, chronic myelogenous leukemia K-562, lymphoblastic leukemia MOLT-4, Burkitt's lymphoma Raji, colorectal adenocarcinoma, lung carcinoma A549, and melanoma G-361 cells (Fig. 3*A*). A recent study showed that these tumorigenic cell lines express hIKCa1 channel mRNA (44). Thus, the presence of *hSK2* seems to be specific to the leukemic Jurkat T cells.

The phylogenetic relationships of 23 different SK and IK channel GenBank™ entries and of *hSK2* were examined (Fig. 4*A*). The amino acid sequence alignment of the complete open reading frames of all 23 genes was performed using the software ClustalX. The unrooted phylogenetic tree was constructed by the neighbor-joining method after exclusion of gaps. The tree file was plotted using the software NJplot. Horizontal branch lengths are drawn to scale, with the *bar* indicating 0.05 amino acid substitution per site. The SK and IK channel genes are divided into two main clusters, one of the SK channel family and the other of the IK channel family with high bootstrap values Fig. 4*A*). The SK channel family cluster is further subdivided into two clusters with *SK2* and *SK3* isoforms in one cluster and the *SK1* isoforms in the other cluster. The IK family genes are subdivided into two main clusters, with the murine/rodent and human IK genes falling into two different groups (Fig. 4*A*).

Although we did not experimentally examine the human chromosomal localization of *hSK2*, a Blastn search at the GenBank™ via the HTGS identified three matching human chromosome 5 contigs (AC010595, AC021085, and AC025761), suggesting that *hSK2* maps to human chromosome 5. Furthermore, we performed an electronic PCR scanning the sequence of these three chromosome 5 contigs in dbSTS data base. The contigs AC021085 and AC025761 retrieved one STS, D5S2065 (GenBank™ accession number Z54068). On the Marshfield map, D5S2065 is mapped to chromosome 5 at position 122.01 (centimorgan). On the WI-YAC and genethon maps, D5S2065 is assigned to chromosome 5 at positions 389 (ordinal) and 121.70 (centimorgan), respectively. On the cytogenetic map, the D5S2065 STS is mapped to chromosome 5 between the cytogenetic markers 5q21.2 and 5q22.1 (Fig. 4*B*). In the vicinity of this locus, are found the genes encoding the polysia-

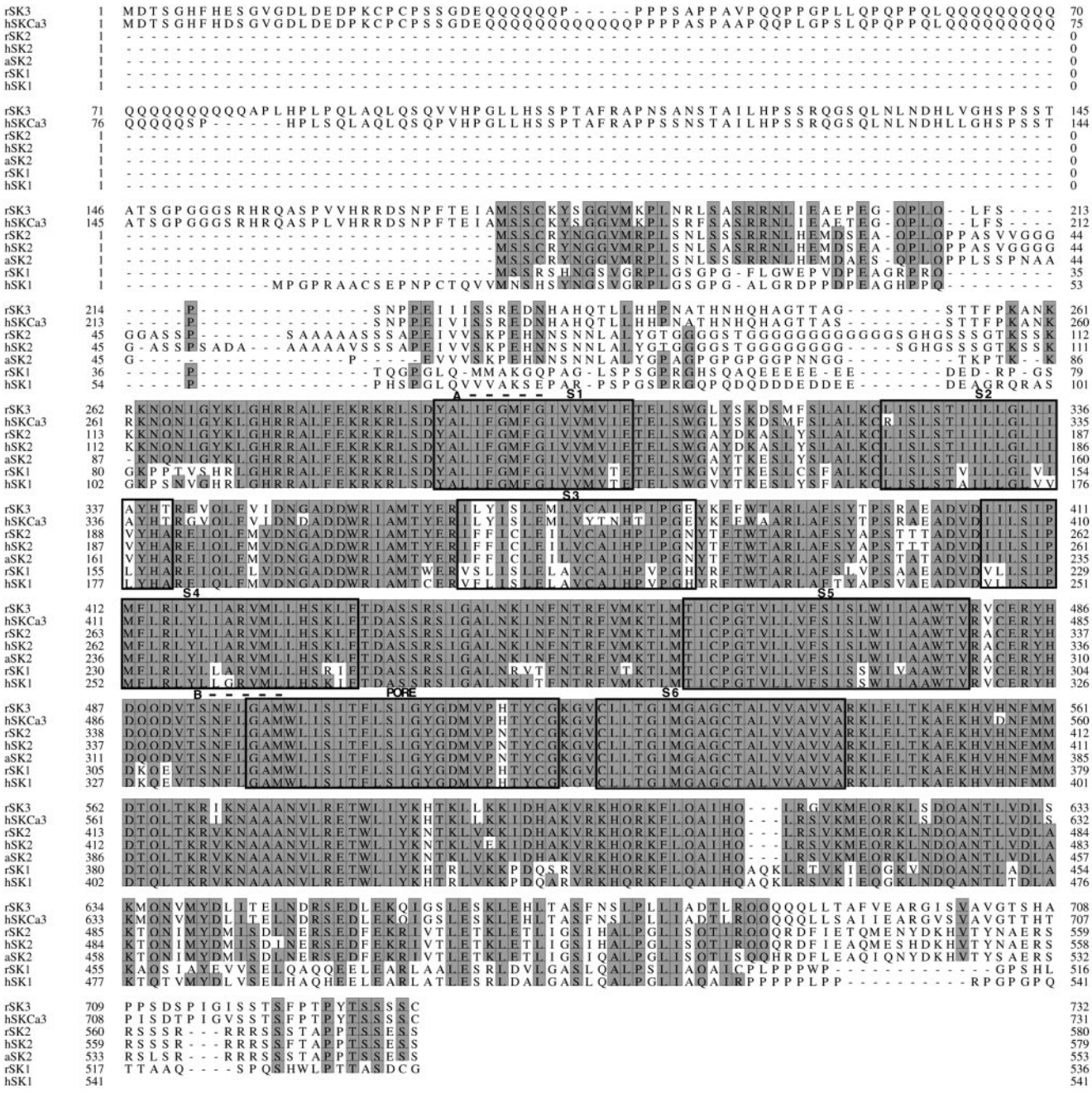

FIG. 2. **Amino acid sequence alignment of hSK2 with *rSK2, aSK2, hSK3, rSK3, hSK1*, and *rSK1*.** Sequences were aligned using ClustalW 1.7 at the BCM search launcher using the default parameters. Gaps are represented by a *dash*. The putative transmembrane domains (S1-S6) and the pore region are *boxed*. Identical residues are shaded *gray*. Positions of the initial degenerate primers *A* and *B*, used for RT-PCR cloning of hSK2 from Jurkat cell mRNA, are indicated as *dashed lines above* the corresponding sequence.

lytransferase, mannosidase, the fer tyrosine kinase, Ca^{2+}-calmodulin kinase type IV, and the adenomatous polyposis coli gene which is responsible for colorectal cancers. However, in the OMIM map no obvious diseases seem to be linked to the *hSK2*/*KCNN2* locus.

Exploiting the high-throughput genome sequence data base and performing a Blast analysis and sequence alignments of the *hSK2* cDNA with the chromosome 5 contigs (AC010595, AC021085, AC025761, AC021415, and AC009589), we could ascertain the genomic organization of the *hSK2*/*KCNN2* gene (Fig. 4, *C* and *D*). Analysis of these clones shows that *hSK2*/*KCNN2* is encoded by 8 exons, with 4 intron-exon junctions within the core domain and 3 intron-exon boundaries at the C terminus of the hSK2 channel sequence (Fig. 4, *C* and *D*).

Functional Expression of hSK2—To study the functional properties of *hSK2*, we transfected either CHO or HEK 293 cells with an expression vector encoding only the *hSK2* coding region. Fig. 5*B* shows typical macroscopic current traces obtained from a CHO cell, patched with 0.96 μM free Ca^{2+} in the pipette solution, and 5 mM K^+ in the bath medium (physiological solution). Under these conditions, a time- and voltage-independent outward K^+ current was elicited by depolarizing test pulses from −120 to +40 mV from a −85 mV holding potential (Fig. 5*B*). Similar results were obtained in HEK 293 cells (not shown). In extracellular high K^+ solutions (165 mM K^+), voltage ramps evoked quasi-linear hSK2 currents with weak inward rectification at positive potentials (Fig. 5*C*). A similar inward rectification was also observed for rSK2 expression in HEK 293 cells (37). A few minutes after break-in to the whole cell configuration, the hSK2 current has the tendency to

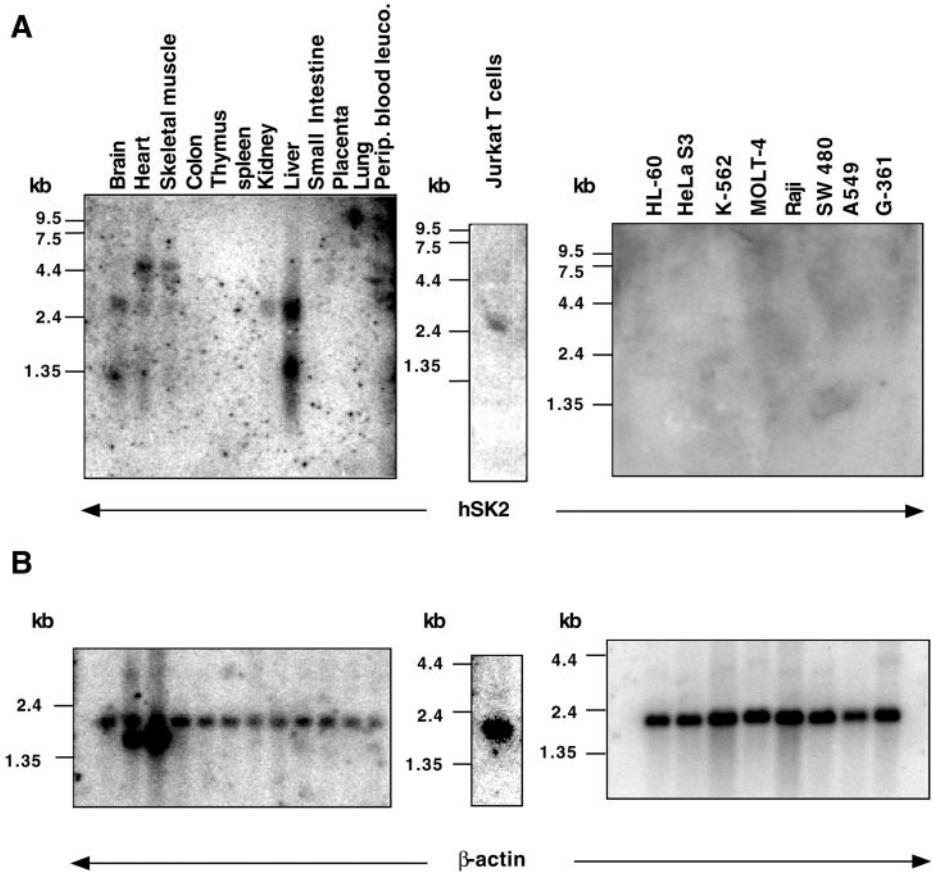

FIG. 3. **Northern blot analysis of *hSK2* transcripts.** *A*, a 5′ specific *hSK2* probe which consisted in the whole 456-bp 5′-UTR was used for the Northern blot analysis in different human tissues (*left panel*), in Jurkat T cells (*middle panel*), and different tumorigenic cell lines (*right panel*). *B*, a human β-*actin* probe was used as a standard positive control to re-probe the blots after stripping for input mRNA.

run-up over time for more than 2-fold (Fig. 5*C*). This slow increase in SK2 current is not caused by an increase in leak conductance and occurs for time periods which exceed by far that needed for diffusion of free Ca^{2+} from the pipette solution to the cell. This current run-up has been also observed for hSK1 and rSK2 channels expressed in HEK 293 cells (37), however, the mechanism underlying this phenomenon is presently unclear. In the absence of Ca^{2+} in the pipette solution, no SK current could be produced (Fig. 5*F*). The reversal potential of the current shifted by 59 mV per 10-fold change in external K^+ concentration, in close agreement with the predicted value of the Nernst equation for a K^+ selective current. The E_{rev} were $+2.2 \pm 0.4$ mV ($n = 5$), -35.6 ± 0.3 mV ($n = 7$) and -86.2 ± 1.0 mV ($n = 9$) at 155, 40, and 5 mM $[K^+]_o$, respectively. In line with the pharmacological characteristics of the SK current expressed by Jurkat T cells (17) and that evoked by expression of the cloned rSK2 channel (29, 30, 37), *hSK2* cDNA expressed a K^+ current that was sensitive to block by apamin (5 nM), scyllatoxin (0.5 nM), and dTC (10 μM) with 78, 54, and 64% of current inhibition, respectively (Fig. 5, *D-F*). The hSK2 current was insensitive to block by CTX or DTX (not shown).

We determined next, the unitary conductance and the calcium dependence of the hSK2-induced K^+ currents in transfected CHO cells (Fig. 6). Using inside-out patches, we found that the single-channel conductance of hSK2 is 9.5 ± 0.7 pS ($n = 5$) (Fig. 6, *B* and *C*), a value very close to that obtained previously for recombinant rSK2 (30). The Ca^{2+} sensitivity of hSK2 was obtained from inside-out macropatches and the Hill plot derived $K_{0.5} = 0.70 \pm 0.02$ μM ($n = 5$), with a steep Ca^{2+} dependence (Hill coefficient $= 4.7 \pm 0.8$, $n = 5$) (Fig. 6*A*).

Regulation of hSK2 in Jurkat T Cells—Activation of normal human T lymphocytes was previously shown to enhance at different extents, expression of both Kv and KCa channel activity (20). Thus, we checked whether hSK2 channels were modulated upon activation of Jurkat T cells at the transcriptional, translational, and functional levels. The *hSK2* expression was compared with that of Kv1.3 channels under the same experimental conditions. Using RT-PCR, cDNA fragments of 797- and 445-bp lengths were specifically amplified from *hSK2* and *Kv1.3* mRNAs, respectively (Fig. 7*A*). In some cases, a nonspecific band of about 600 bp was also amplified using the *hSK2* primers (Fig. 7*A*). Following activation of Jurkat cells for 14 h either by phytohemagglutinin A (PHA, 10 μg/ml) or by the phorbol ester TPA (0.1 μM) + ionomycin (1 μM), there was, respectively, $46 \pm 5\%$ ($n = 3, p < 0.01$) and $69 \pm 4\%$ ($n = 3, p < 0.01$) down-regulation of *hSK2* mRNA as measured by quantitative RT-PCR (Fig. 7, *A* and *B*). A corresponding $54 \pm 9\%$ reduction in SK2 current amplitude is observed after treatment of Jurkat cells with TPA + ionomycin for 14 h ($n = 10, p < 0.01$) (Fig. 8, *C* and *D*). Treatment of TPA alone (0.1 μM) reduces to a slightly higher extent *hSK2* mRNA levels when compared with treatment with ionomycin alone (1 M), with 65 ± 9 and $51 \pm 4\%$ down-regulation, respectively (Fig. 7, *A* and *B*). At the protein level, a similar down-regulation of a specific 57-kDa hSK2 immunoreactive band is observed upon treatment of Jurkat cells with PHA (10 μg/ml) and TPA (0.1 μM) + ionomycin (1 μM) (Fig. 8*A*). Paralleling the regulation at *hSK2* mRNA levels, treatment of Jurkat cells with TPA alone produces a stronger reduction in hSK2 immunoreactive protein than that induced by treatment with ionomycin alone (Fig. 8*A*). In agreement with Northern blot analysis, no *hSK2* mRNA could be detected by RT-PCR neither in resting nor in activated peripheral human T cells (Fig. 7*C*).

In contrast to *hSK2*, *Kv1.3* mRNA and immunoreactive protein are not down-regulated by PHA treatment (10 μg, 14 h) of Jurkat cells (Fig. 7, *A* and *B,* and Fig. 8*A*). PHA does not affect as well the Jurkat Kv currents (not shown). However, treatments with TPA and ionomycin either separately or in combi-

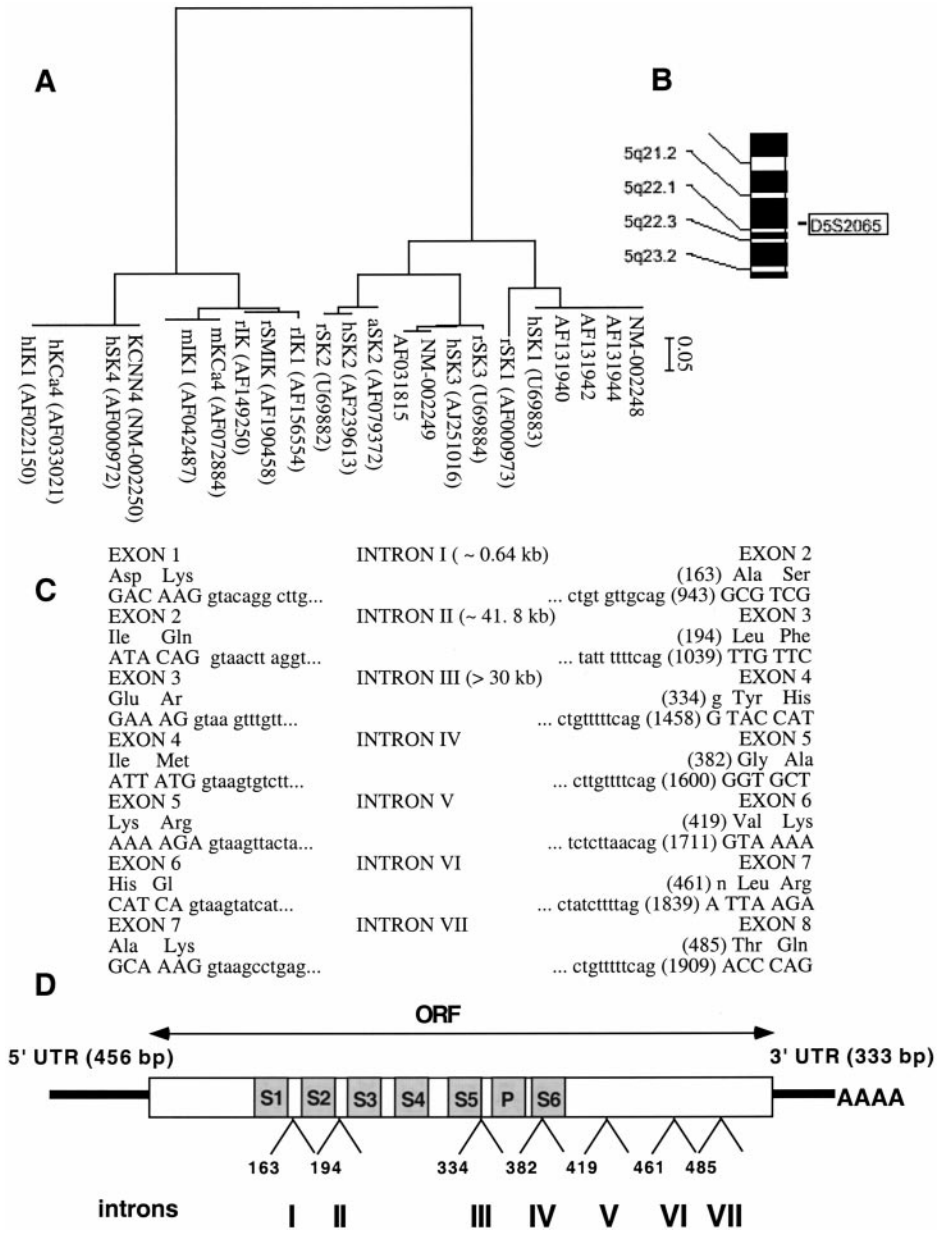

FIG. 4. **Phylogenetic tree, chromosomal localization, and genomic organization of the *hSK2* gene.** *A*, the phylogenetic tree of different SK and IK channel GenBank™ entries and of *hSK2* was constructed by aligning the amino acid sequence of all genes using the software ClustalX and the neighbor-joining method after exclusion of gaps. The tree file was plotted using the software NJplot. The *scale bar* indicates 0.05 amino acid substitution per site. *B*, human chromosomal localization was deduced by retrieving human chromosome 5 contigs (AC010595, AC021085, and AC025761) from the HTGS. The contigs AC021085 and AC025761 retrieved through electronic PCR, one STS, D5S2065 (GenBankTM accession number Z54068). On the cytogenetic map, the D5S2065 STS is mapped to chromosome 5 between the cytogenetic markers 5q21.2 and 5q22.1. *C*, the intron-exon junctions are shown with the corresponding flanking amino acids and genomic sequences. The consensus GT (donor)-AG (acceptor) splice sites are found at each junction. *Numbers* in *parentheses* at the acceptor side refer to amino acid positions and nucleotide positions in the *hSK2* cDNA. *D*, genomic organization ascertained by analysis of contigs (AC010595, AC021085, AC025761, AC021415, and AC009589) from HGTS data base. The *hSK2* mRNA is shown, with 5′- and 3′-UTR as *bold lines*. Within the ORF, transmembrane segments are drawn as *gray boxes*. Introns are shown as *roman numbers*. At each exon-intron junction, the indicated number correspond to the amino acid position at which the exon is flanked by the intron boundary.

nation produce like for *hSK2*, a down-regulation of about 50% of Kv1.3 channels at the mRNA, protein, and functional levels (Fig. 7, *A* and *B,* and Fig. 8, *A* and *C*).

The kinase p56^{lck} is the main non-receptor tyrosine kinase of the Src-like family expressed in Jurkat T cells and it was shown that the p56^{lck}-mediated phosphorylation of the Kv1.3 K^+ channel α subunit is correlated with an inhibition of Kv currents upon Fas stimulation (45). We examined the transcriptional and functional expression of hSK2 channels in normal and p56^{lck}-deficient Jurkat cells (LCK^- cells) and found no significant difference in the levels of *hSK2* steady-state mRNAs as measured by quantitative RT-PCR (Fig. 9, *C* and *D*). The amplitude of the apamin-sensitive SK current was very similar in LCK^- cells and in normal Jurkat cells (Fig. 9, *A* and *B*). Interestingly, restoration and overexpression of p56^{lck} tyrosine kinase (LCK^+ cells) into p56^{lck}-deficient Jurkat cells produced more than 3.5-fold increase in apamin-sensitive SK currents as compared with normal Jurkat or to LCK^- cells (Fig. 9, *A* and *B*). The increase in SK current observed in LCK^+ cells was specific, as the Kv current amplitude remained the same in normal Jurkat, in LCK^- and LCK^+ cells (Fig. 9*E*). The marked up-regulation of SK current in LCK^+ cells was accompanied by

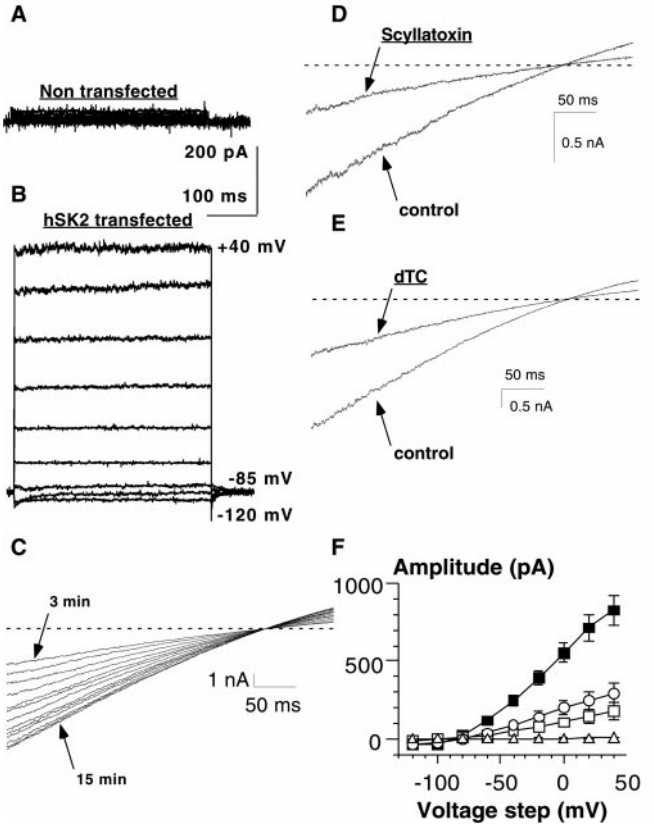

FIG. 5. **Expression of *hSK2* in transfected CHO cells.** *A* and *B,* whole cell currents were recorded in physiological solutions from non-transfected (*A*) and hSK2-transfected (*B*) CHO cells. From a holding potential of −85 mV, the membrane potential was stepped for 400 ms from −120 to +40 mV in 20 mV increments. *C*, representative ramp current recorded from a hSK2-transfected CHO cell at a holding potential of 0 mV in external high K^+ solutions, by a ramp of 340 ms from −130 to +40 mV. To illustrate the run-up of hSK2 current, consecutive ramps are shown from 3 min up to 15 min following break-in to the whole cell configuration. *D* and *E,* representative ramp currents recorded as in *C* before and after application of 0.5 nM scyllatoxin (*D*) and 10 μM dTC (*E*). *F,* current-voltage relationships for control untransfected (*solid squares*, $n = 9$), hSK2-transfected cells with no Ca^{2+} in the pipette solution (*empty triangles*, $n = 5$), and hSK2-transfected cells with 1 μM free Ca^{2+} in the pipette solution which have been treated with 5 nM apamin (*open squares*, $n = 9$) or 10 μM dTC (*open circles*, $n = 8$). The voltage protocol is as in *A* and *B*.

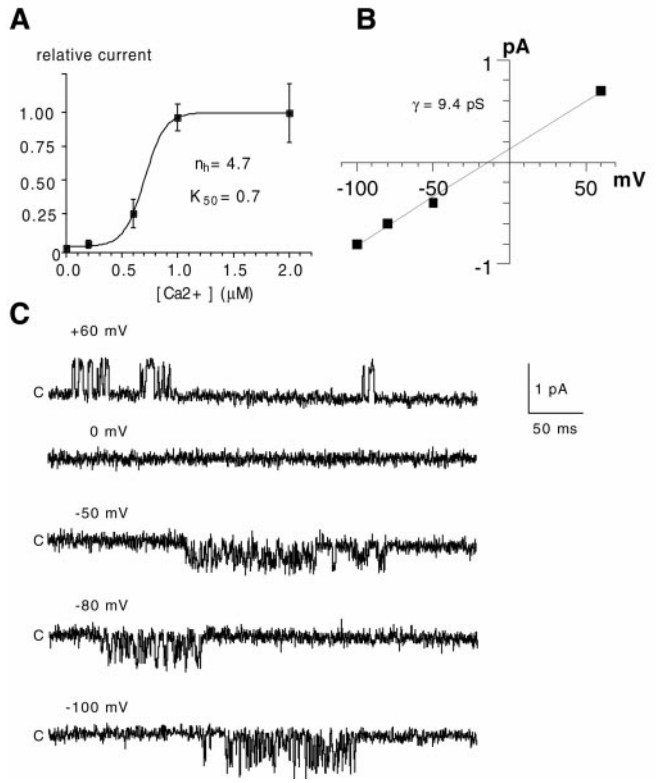

FIG. 6. **Single-channel conductance and calcium sensitivity of hSK2 channels.** *A*, calcium sensitivity of hSK2 currents was determined from inside-out macropatches in the presence of the indicated intracellular free Ca^{2+} concentrations; currents were measured at −140 mV and normalized to that activated at saturating free Ca^{2+} concentrations. Relative current amplitude is plotted as a function of the internal free Ca^{2+} concentration and the data were fitted with the Hill equation. *B*, single-channel activity from a representative inside-out patch, recorded in the presence of 0.7 μM free Ca^{2+} at +60, 0, −50, −80, and −100 mV. *C*, single-channel current-voltage relation for the patch shown in *B*. Data points were derived from single channel amplitudes obtained by the fitting of a single Gaussian function to amplitude histograms. Linear regression yielded a unitary conductance of $\gamma = 9.4$ pS. With the recording solutions (see "Experimental Procedures"), the calculated $E_{rev} = -7$ mV.

a significant increase (70 ± 10%, $n = 3$, $p < 0.01$) in *hSK2* mRNA levels as revealed by RT-PCR (Fig. 9, *C* and *D*).

DISCUSSION

In this work, we have identified the apamin-sensitive KCa channel of human leukemic Jurkat T cells as *hSK2*, the human isoform of the previously cloned rat *SK2* (30). The *hSK2* gene is encoded by 8 exons and could be assigned to chromosome 5 (q21.2-q22.1). In transfected CHO cells, *hSK2* produces a time- and voltage-independent Ca^{2+}-activated K^+ current with a unitary conductance of 9.5 pS and a K_{50} for calcium of 0.7 μM. Like in Jurkat T cells, recombinant hSK2 current is inhibited by apamin, scyllatoxin, and dTC. In contrast to IKCa channels which are transcriptionally induced upon activation of normal human T cells, our results indicate that in Jurkat T cells, SK2 channels are constitutively expressed and are down-regulated following mitogenic stimulation. In Jurkat cells overexpressing the Src family tyrosine kinase $p56^{lck}$ (LCK^+), the SK2 channel activity increases by more than 3-fold.

Human peripheral T lymphocytes express two types of K^+ channels, the Kv channels activated by membrane depolarization and KCa channels which open following an increase in intracellular free Ca^{2+} (20). Kv1.3 channels were found to underlie lymphocytic Kv currents while more recently, hSK4 channels (also called hIK1, hIKCa1, or hKCa4) were shown to account for the CTX-sensitive T cell KCa currents, also called IK or intermediate conductance (25–27, 33). Similarly, the human leukemic Jurkat T cells express two different types of K^+ channels, the Kv and KCa channels. However, contrary to normal T cells, the Jurkat KCa channel exhibits a smaller unitary conductance and a different pharmacology (16, 17).

While the *Kv1.3* gene was shown to encode the Jurkat Kv channels (21), the Jurkat KCa current has been identified recently as *SK2*, based on the PCR amplification of a partial Jurkat *SK2* cDNA fragment (29). Here, we cloned from Jurkat T cells a 2.5-kb full-length cDNA, *hSK2*, encoding the human isoform of SK2 channels. Similar to native Jurkat KCa currents, *hSK2* produces in transfected CHO cells a time- and voltage-independent K^+ current which is sensitive to apamin, scyllatoxin, and dTC and is insensitive to CTX and DTX. The unitary channel conductance of hSK2 is 9.5 pS, a value very close to that obtained previously for recombinant *rSK2* (30). However, it is noteworthy that the recombinant hSK2 unitary conductance is somewhat larger than that determined by fluctuation analysis for the native Jurkat SK channel (4–7 pS) (16). This difference may be accounted for by the different methods of analysis used and the experimental conditions, or

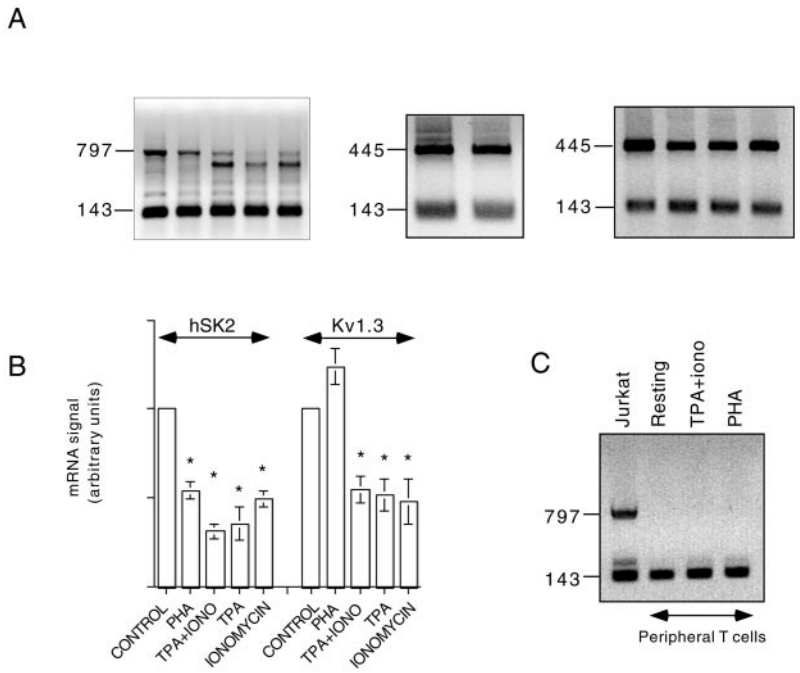

FIG. 7. **Modulation of *hSK2* and *Kv1.3* mRNAs following mitogenic stimulation of Jurkat cells.** *A,* representative experiment illustrating quantitative RT-PCR performed to detect changes in *hSK2* and *Kv1.3* mRNAs following mitogenic stimulation (14 h) of Jurkat T cells by PHA (10 μg/ml) or by 0.1 μM TPA and 1 μM ionomycin, either alone or in combination as indicated. Primers spanning the nucleotides 1624–2421 of *hSK2* cDNA and the nucleotides 460–905 of *hKv1.3* cDNA (21), amplified respectively, a 797-bp *hSK2* and a 445-bp *hKv1.3* PCR fragments. The co-amplification of an internal control housekeeping gene, the human *S14* ribosomal protein mRNA was performed as described (47) and amplified a 143-bp PCR fragment. Equal aliquots of each PCR were removed and analyzed by 1.2% agarose gel electrophoresis. *B*, data were quantified by scanning the labeled bands and normalized to the 143-bp S14 signal. Values are expressed as mean ± S.E. (n = 3–5, * $p < 0.01$). *C,* no *hSK2* mRNA could be detected in resting or activated human peripheral T cells (PHA 10 μg/ml, 48 h; or 0.1 μM TPA + 1 μM ionomycin, 48 h).

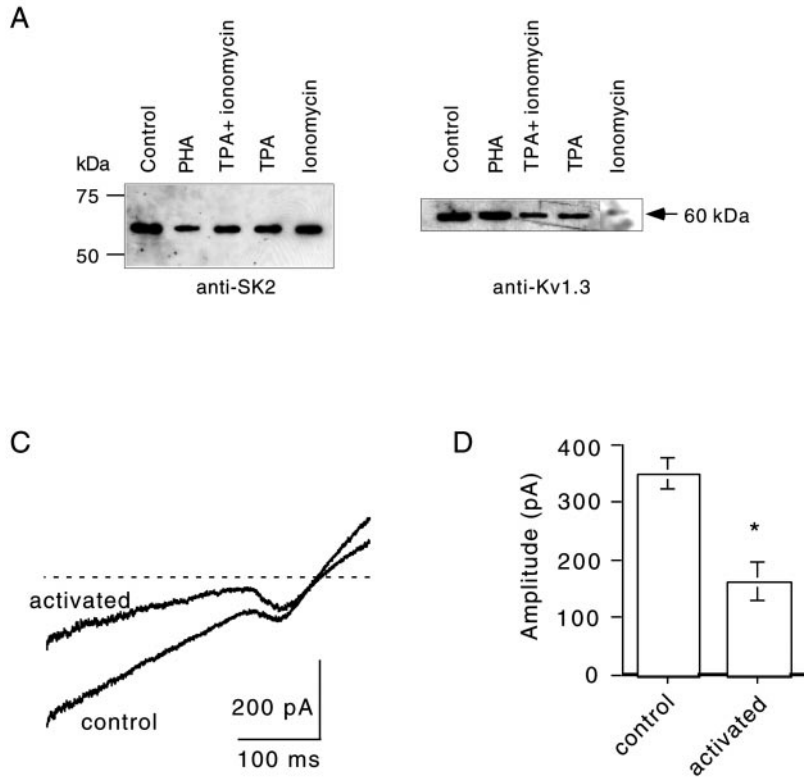

FIG. 8. **Modulation of hSK2 and Kv1.3 channel proteins and currents following mitogenic stimulation of Jurkat cells.** *A*, representative Western blots illustrating the changes in hSK2 and Kv1.3 immunoreactive proteins following mitogenic stimulation (14 h) of Jurkat T cells by PHA (10 μg/ml) or 0.1 μM TPA and 1 μM ionomycin, either alone or in combination as indicated. hSK2 and Kv1.3 immunoreactive proteins were detected as 57- and 60-kDa bands, respectively, using polyclonal anti-rSK2 and anti-hKv1.3 antibodies. *C*, representative ramp currents recorded from control and activated (0.1 μM TPA + 1 μM ionomycin, 14 h) Jurkat cells. Currents were recorded from a holding potential of 0 mV in external high K^+ solutions by a ramp of 400 ms from −160 to +40 mV. *D*, statistics of the experiments as in *C*. SK2 currents are significantly reduced following TPA + ionomycin treatment (n = 13, * $p < 0.01$).

by the existence of an auxilary subunit in Jurkat cells. The Ca^{2+} sensitivity of hSK2 provides a $K_{0.5}$ of 0.7 μM, with a steep Ca^{2+} dependence (η = 4.7), which is in line with the values previously reported for rSK2 (30).

The protein encoded by *hSK2* is highly homologous to its rat protein counterpart *rSK2* with 97% identity (30). Although we did not experimentally examine the human chromosomal localization of *hSK2*, a Blastn search at the GenBank™ via the HTGS identified three matching human chromosome 5 contigs (AC010595, AC021085, and AC025761), which retrieved one

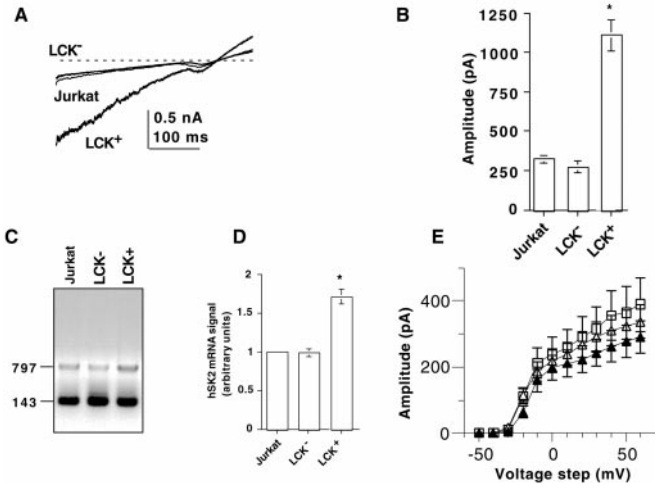

FIG. 9. **SK2 and Kv1.3 currents in Jurkat, LCK$^-$ and LCK$^+$ cells.** *A*, representative ramp currents recorded in normal (Jurkat), p56^{lck}-deficient (LCK$^-$) and overexpressed p56^{lck} Jurkat cells (LCK$^+$). Currents were recorded from a holding potential of 0 mV in external high K^+ solutions by a ramp of 400 ms from −160 to +40 mV. *B,* statistics of the experiments as in *A*. SK2 current amplitude as determined at −160 mV was significantly increased in LCK$^+$ cells as compared with Jurkat cells ($n = 21$, * $p < 0.001$). *C*, representative experiment illustrating quantitative RT-PCR performed as in Fig. 7*A*, to detect differences in *hSK2* mRNAs in Jurkat, LCK$^-$, and LCK$^+$ cells. *D*, data were quantified by scanning the labeled bands and normalized to the 143-bp S14 signal. Values are expressed as mean ± S.E. Higher levels of *hSK2* mRNAs are seen in LCK$^+$ cells as compared with LCK$^-$ and Jurkat cells ($n = 3$, * $p < 0.01$). *E*, current-voltage relations of Kv1.3 recorded in physiological solutions in Jurkat (*open squares*, $n = 9$), LCK$^-$ (*open triangles*, $n = 9$), and LCK$^+$ (*solid triangles*, $n = 10$) cells.

STS, D5S2065. This analysis allowed us to assign the *hSK2*/*KCNN2* gene to human chromosome 5 (q21.2-q22.1) and to ascertain the genomic organization of *hSK2*. Although SK and IK channel genes are subdivided into different clusters on the phylogenetic tree (see Fig. 4*A*), there is a remarkable similarity in intron-exon boundary location if one compares our hSK2 data with those recently published for *IKCa1* and *SKCa1–3* genes (44), suggesting a common ancestral gene. It is also noteworthy that like the *IKCa1* mRNA, the *hSK2* mRNA comprises short 5′- and 3′-untranslated regions (456 and 333 bp, respectively).

Our data indicate substantial differences between KCa channels of normal human T lymphocytes and leukemic Jurkat T cells. 1) In terms of their molecular entities as they are encoded by two different genes, *hSK4* (or *hIK1, hIKCa1*, and *hKCa4*) (25–27, 33) and *hSK2* (the present work), respectively. 2) In terms of their basal expression at rest and their regulation following mitogenic stimulation. Resting normal human T cells express on average ~8 hIKCa channels/cell, along with ~300 Kv1.3 channels/cell, while resting Jurkat cells express on average ~400 SK channels and 400 Kv1.3 channels (16, 20, 44). A number of studies have shown that activation of normal human T cells potently induces KCa channel activity which is accompanied by the transcriptional induction of *hSK4*/*hIKCa1* mRNAs (27, 33, 44). *IKCa1* expression increases from an average of 8 to 300–800 channels per cell following mitogenic activation of normal human T cells and mitogens enhance *IKCa1* promoter activity via AP1 and Ikaros-2 motifs (44). Our results show that in Jurkat T cells, there is constitutive expression of hSK2 channels as we determined at the mRNA, protein, and functional levels. There is also constitutive expression of Kv1.3 channels. Following activation of Jurkat T cells by PHA, there is neither up-regulation of SK currents nor transcriptional induction of hSK2 mRNA. Rather, there is a significant decrease in *hSK2* transcript and protein, paralleled by a marked down-regulation of SK currents. In Jurkat cells, while hSK2 channels are down-regulated by PHA, TPA, and to a lesser extent by ionomycin, Kv1.3 channels appear to be insensitive to PHA treatment and are reduced only by TPA and ionomycin exposures. Thus, Jurkat T cells appear anomalous in their constitutive expression of hSK2 channels. In normal human T cells, Kv1.3 channels appear essential for activation of resting cells, while activated cells require IKCa channels for the reactivation response (23, 33, 44). It is likely that the mechanisms governing the regulation of KCa channel activity following normal T cell activation have been disrupted in Jurkat cells since they are leukemic cells which have lost the control of proliferation. It is possible that the marked down-regulation of hSK2 and Kv1.3 channels produced by mitogenic stimulation of Jurkat cells serves as a negative feedback to limit the activity of potassium channels (KCa and Kv) in order to restrict proliferation of these leukemic cells. However, Jurkat SK channels may also contribute to the positive feedback control between cytosolic Ca^{2+} and membrane potential and both Kv and KCa channel activities were suggested to sustain Ca^{2+} oscillations in Jurkat cells (16).

The marked increase in SK currents (more than 3.5-fold) following overexpression of p56^{lck} tyrosine kinase in LCK$^+$ cells seems to involve a transcriptional up-regulation. In preliminary experiments, pretreatment of LCK$^+$ cells with genistein (100 μM) did not affect the SK current.[2] However, a modulation of hSK2 channels by phosphorylation should not be excluded. The increase in SK currents is specific since the levels of Kv channel activity appear to be similar in Jurkat, LCK$^-$, and LCK$^+$ cells. Recent work suggests that ceramide via p56^{lck} kinase regulates Kv1.3 channel activity upon Fas stimulation (45, 46). It will be important to check in future experiments the possible direct modulation of *hSK2* by p56^{lck} tyrosine kinase and to examine by analogy whether such regulations occur for hSK4/hIKCa channels in normal human T lymphocytes.

Acknowledgments—We thank Prof. Arthur Weiss (University of California at San Francisco) for providing the p56^{lck}-deficient and p56^{lck}-overexpressing Jurkat cells, Dr. Amanda Patel for the gift of pIRES-CD8, Sarah Etkin for skillful technical assistance, and Dr. Ronen Alon for constructive discussions.

REFERENCES

1. Blatz, A., and Magleby, K. (1987) *Trends Neurosci.* **10,** 463–467
2. Sah, P. (1996) *Trends Neurosci.* **19,** 150–154
3. Vergara, C., Latorre, R., Marrion, N., and Adelman, J. P. (1998) *Curr. Opin. Neurobiol.* **8,** 321–329
4. Romey, G., Hugues, M., Schmid-Antomarchi, H., and Lazdunski, M. (1984) *J. Physiol.* **79,** 259–264
5. Moczydlowski, E., Lucchesi, K., and Ravindran, A. (1988) *J. Membr. Biol* **105,** 95–111
6. Castle, N., Haylett, D. G., and Jenkinson, D. H. (1989) *Trends Neurosci.* **12,** 59–65
7. Strong, P. N. (1990) *Pharmacol. Ther.* **46,** 137–162
8. Hugues, M., Duval, D., Kitabgi, P., Lazdunski, M., Vincent, J.-P. (1982) *J. Biol. Chem.* **257,** 2762–2769
9. Hugues, M. (1982) *Biochem. Cell Biol. Commun.* **107,** 1577–1582
10. Hugues, M., Duval, D., Schmid, H., Kitabgi, P., Lazdunski, M., and Vincent, J. P. (1982) *Life Sci.* **31,** 437–443
11. Hugues, M., Schmid, H., Romey, G., Duval, D., Frelin, C., and Lazdunski, M. (1982) *EMBO J.* **1,** 1039–1042
12. Hugues, M., Romey, G., Duval, D., Vincent, J. P., and Lazdunski, M. (1982) *Proc. Natl. Acad. Sci. U. S. A.* **79,** 1308–1312
13. Lazdunski, M., Fosset, M., Hughes, M., Mourre, C., Romey, G., and Schmid-Antomarchi, H. (1985) *Biochem. Soc. Symp.* **50,** 31–42
14. Mourre, C., Hugues, M., and Lazdunski, M. (1986) *Brain Res.* **382,** 239–249
15. Schmid-Antonmarchi, H., Hugues, M., and Lazdunski, M. (1986) *J. Biol. Chem.* **261,** 8633–8637
16. Grissmer, S., Lewis, R. S., and Cahalan, M. D. (1992) *J. Gen. Physiol.* **99,** 63–84
17. Hanselmann, C., and Grissmer, S. (1996) *J. Physiol.* **496,** 627–637
18. Wadsworth, J. D., Torelli, S., Doorty, K. B., and Strong, P. N. (1997) *Arch.*

[2] Desai, A. Peretz, B. Attal, unpublished data.

Biochem. Biophys. **346,** 151–160
19. Pribmow, D., Johnson-Pais, T., Bond, C. T., Keen, J., Johnson, R. A., Janowsky, A., Silvia, C., Thayer, M., Maylie, J., and Adelman, J. P. (1999) *Muscle & Nerve* **22,** 742–750
20. Lewis, R. S., and Cahalan, M. D. (1995) *Annu. Rev. Immunol* **13,** 623–653
21. Attali, B., Romey, G., Honore, E., Schmid-Alliana, A., Mattei, M. G., Lesage, F., Ricard, P., Barhanin, J., and Lazdunski, M. (1992) *J. Biol. Chem.* **267,** 8650–8657
22. Cai, Y. C., Osborne, P. B., North, R. A., Dooley, D. C., and Douglass, J. (1992) *DNA Cell Biol.* **11,** 163–172
23. Grissmer, S., Nguyen, A. N., and Cahalan, M. D. (1993) *J. Gen. Physiol.* **102,** 601–630
24. Verheugen, J. A. H., Vijverberg, H. P. M., Oortgiesen, M., and Cahalan, M. D. (1995) *J. Gen. Physiol.* **105,** 765–794
25. Joiner, W. J., Wang, L. Y., Tang, M. D., and Kaczmarek, L. K. (1997) *Proc. Natl. Acad. Sci. U. S. A.* **94,** 11013–11018
26. Ishii, T. M., Silvia, C., Hirschberg, B., Bond, C. T., Adelman, J. P., and Maylie, J. (1997) *Proc. Natl. Acad. Sci. U. S. A.* **94,** 11651–11656
27. Logsdon, N. J., Kang, J., Togo, J. A., Christian, E. P., and Aiyar, R. J. (1997) *J. Biol. Chem.* **272,** 32723–32726
28. Jensen, B. S., Strobaek, D., Christophersen, P., Jorgensen, T. D., Hansen, C., Silahtaroglu, A., Olesen, S. P., and Ahring, P. K. (1998) *Am. J. Physiol.* **275,** C848–C856
29. Jager, H., Adelman, J. P., and Grissmer, S. (2000) *FEBS Lett.* **469,** 196–202
30. Kohler, M., Hirschberg, B., Bond, C. T., Kinzie, J. M., Marrion, N. V., Maylie, J., and Adelman, J. P. (1996) *Science* **273,** 1709–1714
31. Xia, X. M., Fakler, B., Rivard, A., Wayman, G., Johnson-Pais, T., Keen, J. E., Ishii, T., Hirschberg, B., Bond, C. T., Lutsenko, S., Maylie, J., and Adelman, J. P. (1998) *Nature* **395,** 503–507
32. Keen, J. E., Khawaled, R., Farrens, D. L., Neelands, T., Rivard, A., Bond, C., Janowsky, A., Fakler, B., Adelman, J. P., and Maylie, J. (1999) *J. Neurosci.* **19,** 8830–8838
33. Khanna, R., Chang, M. C., Joiner, W. J., Kaczmarek, L. K., and Schlichter, L. C. (1999) *J. Biol. Chem.* **274,** 14838–14849
34. Fanger, C. M., Ghanshani, S., Logsdon, N. J., Rauer, H., Kalman, K., Zhou, J., Beckingham, K., Chandy, K. G., Cahalan, M. D., and Aiyar, J. (1999) *J. Biol. Chem.* **274,** 5746–5754
35. Ishii, T. M., Maylie, J., and Adelman, J. P. (1997) *J. Biol. Chem.* **272,** 23195–23200
36. Shah, M., and Haylett, D. G. (2000) *Br. J. Pharmacol.* **129,** 627–630
37. Strobaek, D., Jorgensen, T. D., Christophersen, P., Ahring, P. K., and Olesen, S. P. (2000) *Br. J. Pharmacol.* **129,** 991–999
38. Hamill, O. P., Marty, A., Neher, E., Sakmann, B., and Sigworth, F. J. (1981) *Pflugers Arch.* **391,** 85–100
39. Sobko, A., Peretz, A., and Attali, B. (1998) *EMBO J.* **17,** 4723–4734
40. Jurman, M. E., Boland, L. M., Liu, Y., and Yellen, G. (1994) *BioTechniques* **17,** 876–881
41. Chomczynski, P., and Sacchi, N. (1987) *Anal. Biochem* **162,** 156–159
42. Frohman, M. A. (1995) in PCR Primer, A Laboratory Manual (Dieffenbach, C. W., and Dreksler, G. S., eds) pp. 381–409, Cold Spring Harbor Laboratory Press, Cold Spring Harbor, NY
43. Kozak, M. (1987) *Nucleic Acids Res.* **15,** 8125–8148
44. Ghanshani, S., Wulff, H., Miller, M. J., Rohm, H., Neben, A., Gutman, G. A., Cahalan, M. D., and Chandy, K. G. (2000) *J. Biol. Chem.* **275,** 37137–37149
45. Szabo, I., Gulbins, E., Apfel, H., Zhang, X., Barth, P., Busch, A. E., Schlottman, K., Pongs, O., and Lang, F. (1996) *J. Biol. Chem.* **271,** 20465–20469
46. Gulbins, E., Szabo, I., Baltzer, K., and Lang, F. (1997) *Proc. Natl. Acad. Sci. U. S. A.* **94,** 7661–7666
47. Shirihai, O., Merchav, S., Attali, B., and Dagan, D. (1996) *Pflugers Arch.* **431,** 632–638